ELSEVIER

Polymer 41 (2000) 5375–5383

polymer

Phase diagram, morphology development and vulcanization induced phase separation in blends of syndiotactic polypropylene and ethylene–propylene diene terpolymer

A. Ramanujam, K.J. Kim[1], T. Kyu*

Institute of Polymer Engineering, University of Akron, Akron, OH 44325-0301, USA

Received 22 March 1999; received in revised form 24 September 1999; accepted 27 September 1999

Abstract

Miscibility phase diagram in blends of syndiotactic polypropylene (sPP) and ethylene–propylene diene terpolymer has been established by means of differential scanning calorimetry, light scattering and optical microscopy. In descending order of temperature, the olefinic blends reveal a complex phase diagram involving a lower critical solution temperature (LCST), a single phase region followed by a depression of melting transition and a crystal transition (crystallization) of sPP. Below the liquid–solid crystal coexistence line, phase separation occurs in competition with crystallization of sPP in the blends. Temporal evolution of structure factors and the emergence of phase separated domains in these blends have been investigated by time-resolved light scattering and optical microscopy following several temperature quenches from a single phase into the LCST immiscibility gap. The temporal evolution of structure factors has been analyzed in the context of nonlinear dynamical scaling laws. Vulcanization induced phase separation has been undertaken at various temperatures in the single-phase region. Of particular interest is that the higher the reaction temperature (i.e. the faster the chemical reaction), the smaller the domain size.

Keywords: Polyolefin blends; Phase diagram; Lower critical solution temperature

1. Introduction

In recent years, thermoplastic elastomers have gained considerable interest because of their technological significance [1–9]. One of the most commercially successful thermoplastic polyolefin blends is the thermoplastic elastomer mixture composed of polypropylene (PP) and ethylene–propylene diene terpolymer (EPDM) [1–6]. The PP/EPDM blends are known for in-situ cross-linkability afforded by the elastomeric component and melt processability rendered by the thermoplastic component.

In literature [1–6], the melt blends of the commercial grade PP and EPDM are perceived to be immiscible. This perception has changed recently when a lower critical solution temperature (LCST) phase diagram was found in the blends of isotactic polypropylene (iPP) and EPDM [8]. A small miscibility gap existed between the LCST and the crystallization temperatures of iPP in the blends. However, the mutual interference of the crystal melting and liquid–liquid phase separation makes the study on kinetics of reaction induced phase separation difficult [8]. The need for uncoupling the melting and phase separation was recognized in order to confirm the existence of the LCST and to make the kinetic study easier. Syndiotactic polypropylene (sPP) has been sought because of the lower melting temperature (T_m) of sPP (i.e. about 40°C lower than that of iPP) so that the effect of T_m on the LCST phase diagram may be reduced or eliminated completely.

In this paper, phase diagrams of blends of sPP/EPDM have been established by means of differential scanning calorimetry (DSC), light scattering, and optical microscopy. Of particular interest is that the sPP/EPDM blends exhibit an LCST type coexistence curve about 25–35°C above the T_m of sPP. As typical for an LCST, the cloud point phase diagram of the sPP/EPDM blend is thermally reversible. At a lower temperature, an upper critical solution temperature (UCST) seemingly occurs in the vicinity of the sPP crystallization temperature. The competition between thermal-quench induced phase separation and crystallization has been investigated in relation to the emergence

* Corresponding author. Tel.: +1-330-972-6672; fax: +1-330-258-2339.
E-mail address: tkyu@uakron.edu (T. Kyu).
[1] Permanent Address: Department of Textile Engineering, Kyung Hee University, 1 Seochun-ri, Kiheung-eup, Yongin-si, Kyunggi-do 449-701, South Korea.

0032-3861/00/$ - see front matter
PII: S0032-3861(99)00740-5

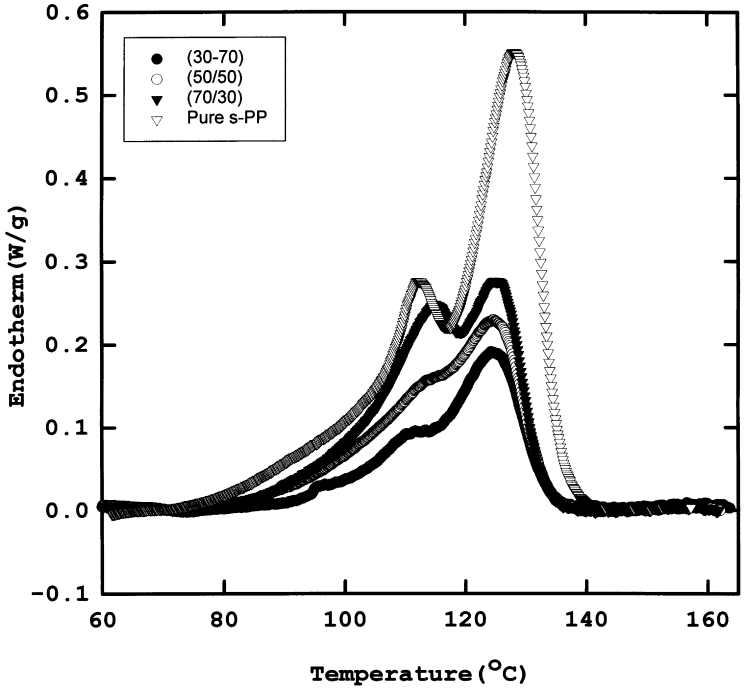

Fig. 1. DSC thermograms of various sPP/EPDM blends, displaying dual melting transitions. The thermograms were obtained from the first heating cycles of the solvent cast blend films. The heating rate was 10°C/min.

of blend morphology. Temporal evolution of structure factors and/or phase separated domains in these blends have been investigated by means of time-resolved light scattering and optical microscopy following several temperature jumps from a single phase to various temperatures within the LCST immiscibility gap. Furthermore, vulcanization induced phase separation (VIPS) was undertaken for various blends of sPP/EPDM in the single-phase temperatures using phenolic resin as a curing agent. The growth behavior of both thermally induced phase separation and of VIPS has been analyzed in the framework of the dynamical scaling laws [10].

2. Experimental section

Syndiotactic polypropylene (sPP) was kindly supplied by Fina Chemical Co. The weight average and the number average molecular weight of sPP were reported to be 174,000 and 74,700, respectively, with a polydispersity of 2.3. EPDM having a moderate level of diene content, i.e. 4–5% of ethylidene norbornene (ENB) and 50% ethylene content in the copolymer was kindly supplied by Exxon Chemical Co. As typical for a commercial material, the EPDM specimen has a broad molecular weight distribution.

Various blends of iPP/EPDM were prepared by first dissolving iPP powders in xylene at 130°C, then EPDM was added after lowering the temperature to 100°C and stirred thoroughly for about 90 min to ensure complete mixing. Film specimens were prepared by solvent casting at ambient temperature in a fume hood and dried in a vacuum oven at room temperature for 48 h. The thickness of the blend films used for light scattering and optical microscopy was approximately 10–20 μm. Flake samples were also prepared by pouring the solution mixture into a non-solvent such as ethanol and washed several times and dried at ambient temperature. The flakes were further dried in a vacuum oven at 50°C for 48 h and then melt pressed in a laboratory hot press at 200°C for 20 min at elevated pressures. In order to remove any trapped bubbles, the pressure was suddenly released and increased again; this procedure was repeated several times.

Melting point depression and glass transition (T_g) of the sPP/EPDM were determined using DSC (Model 9900, Du Pont) inter-linked to the heating module (Model 910, Du Pont). Approximately 10 mg of the blends was encapsulated in DSC pans. The DSC scans were undertaken under nitrogen environment with heating and cooling rates varying from 20 to 2°C/min. Pseudo-equilibrium melting temperatures (T_m°) were estimated by extrapolating the data to zero heating rate. In the T_g measurement, a heating rate of 10°C/min was utilized.

A cloud point measurement was performed using light scattering at a given scattering angle (approximately 10°) with a heating and cooling rate of 0.5°C/min. Time-resolved light scattering was carried out by simultaneous measurement of scattering angles (2θ of 0–40°) using a Reticon camera inter-linked with an Optical Multichannel Analyzer (OMA III) [11]. A polarized light microscope (Nikon Optiphot 2-pol) attached with a Nikon camera (FX-35DX)

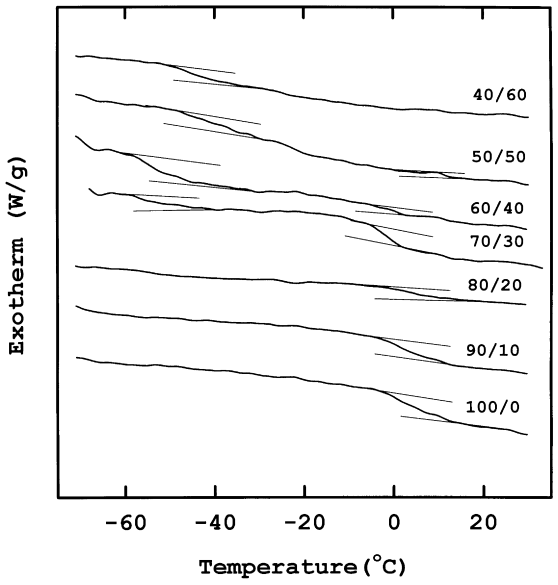

Fig. 2. DSC thermograms showing dual glass transition temperatures corresponding to those of the constituents as a function of composition. The thermograms were obtained from the first heating cycles of the solvent cast blend films. The scan rate was 10°C/min.

was used for identifying the structure evolution. A programmable temperature controller (TMS 93, Linkam) was used along with a sample chamber (LTS 350, Linkam) for heating specimens in microscopic investigations.

Vulcanization of the sPP/EPDM blends was undertaken as various compositions and various temperatures using a phenolic resin as a curing agent. The amount of the phenolic curing agent was 10 parts per 100 of EPDM.

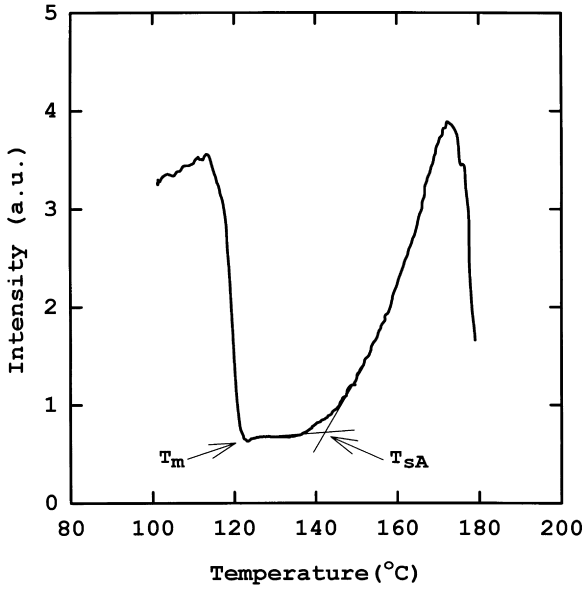

Fig. 3. Change of scattered intensity (at $2\theta = 10°$) during the heating run of the 50/50 sPP/EPDM blend at a heating rate of 1°C/min.

3. Results and discussion

3.1. Miscibility characterization and phase diagram

The melting transitions in blends of sPP and EPDM with low ethylene content were determined by DSC. Fig. 1 depicts typical DSC thermograms for the pure sPP and various sPP/EPDM blends obtained at 10°C/min, displaying dual melting peaks. In general, the revelation of two melting peaks has been attributed either to the presence of two types of crystal modifications of PP undergoing crystal–crystal transformation or melting-recrystallization of one crystal type [12]. The former mechanism is due to the transformation of one type of crystal form to another type of a more stable crystal modification during heating. Well-known examples are the α and γ forms of iPP that undergo solid–solid phase transition. In the latter, the melting peak of the lower temperature side is ascribed to the fusion of the original crystals. The higher melting peak is associated with the melting of the recrystallized ones. These peak positions depend strongly on the competition between the melting of the original crystals and that of the recrystallized ones. The rate dependent DSC study [13] reveals that the dual peaks in the present sPP are a consequence of melting-recrystallization.

To mimic the dependence of glass transition on blend compositions, the DSC scans were carried from −80 to 40°C at a rate of 10°C/min. Fig. 2 shows dual glass transitions corresponding to those of the constituents, suggestive of the immiscible character of the blends at such low temperatures where crystallization of sPP has already occurred in the blends. From the DSC results alone, it is unclear whether sPP and EPDM undergo phase separation prior to crystallization or whether the process of phase separation is induced by crystallization. Nevertheless, there is no doubt that the emergence of phase morphology may be influenced by the competition between phase separation and crystallization.

A light scattering technique was employed to determine the cloud point phase diagram. Fig. 3 exhibits the change of scattered intensity at an arbitrary scattering angle (2θ) of 10° during the course of heating and cooling cycles. The initial decrease of scattered intensity is due to the crystal melting accompanied by homogenization. The intensity remains invariant for some time in the homogeneous melt. With continuing heating the scattered intensity increases, which may be attributed to the occurrence of liquid–liquid phase separation driven by LCST. In the cooling cycle, this phase decomposition process is reversible, except that there was a supercooling effect, showing a hysteresis [8,13]. A similar experiment was undertaken for other blend compositions for determining the loci of the liquid–liquid coexistence curve that resembled an LCST occurring in the melt.

Fig. 4 depicts the coexistence of LCST and UCST cloud point curves of sPP/EPDM blends together with the melting and crystallization transitions of sPP. The pseudo-equilibrium

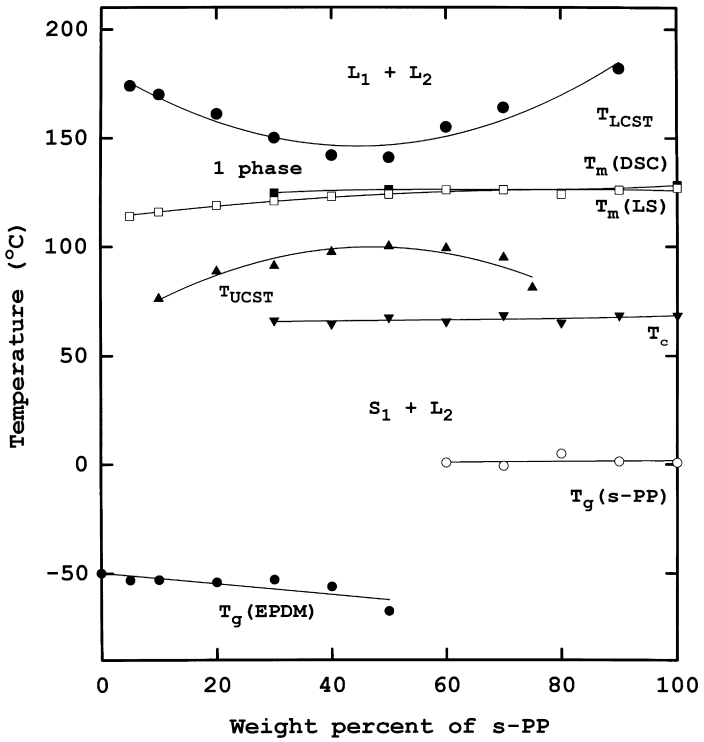

Fig. 4. Phase diagram exhibiting LCST of the sPP/EPDM blends, pseudo-equilibrium melting and crystallization temperatures of sPP in the blends.

melting points (T_m°) were obtained by measuring T_m at various heating rates and subsequently extrapolating to zero heating rate. A similar attempt has been made to estimate the pseudo-equilibrium crystallization temperature, T_c°. However, the determination of the equilibrium-phase transition temperature is usually ambiguous due to the non-equilibrium nature of polymer crystallization (i.e. the strong dependence of crystallization on the cooling rate). Hence, only the rate-dependent crystallization temperatures of sPP as obtained in the DSC studies are included in the phase diagram. The UCST as obtained in the Vv (both polarizers are parallel) scattering experiment is well below the T_m of sPP in the blends, but it is intersected with the non-equilibrium (obtained at 10°C/min) crystallization temperature. It should be noted that the pseudo-equilibrium crystallization temperature (extrapolated to zero heating rate) is generally higher. Nevertheless, a single-phase region can be identified between the LCST and the melting point depression curve.

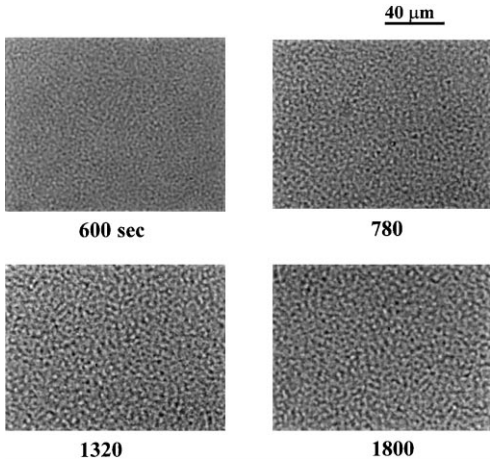

Fig. 5. Spatio-temporal growth of interconnected phase-separated domains during a *T* jump from a single-phase (128°C) to a two-phase temperature of 175°C.

Upon cooling the 50/50 blend of sPP/EPDM from a single phase to room temperature, the scattered intensity increases, which may be attributed to increase in concentration fluctuations during phase separation and/or orientation fluctuations caused by crystallization. Depolarized light scattering is useful in distinguishing these two mechanisms as Vv scattering (both polarizer and analyzer are vertical) arises due to both concentration and orientation fluctuations, whereas Hv scattering (a horizontal polarizer with a vertical analyzer) is very specific to the orientation fluctuations. Experimentally the Vv scattering was found to arise before the Hv scattering [13]. This revelation suggests that there is liquid–liquid phase separation taking place prior to crystallization in the sPP phase. To determine the coexistence curve, a similar Vv scattering experiment was undertaken for other blend compositions. The curvature of the cloud point curve is convex downward, resembling an UCST. Subsequently, crystallization of sPP takes place in the blends.

3.2. Dynamics of thermally induced phase separation

The observed single-phase region permits the investigation

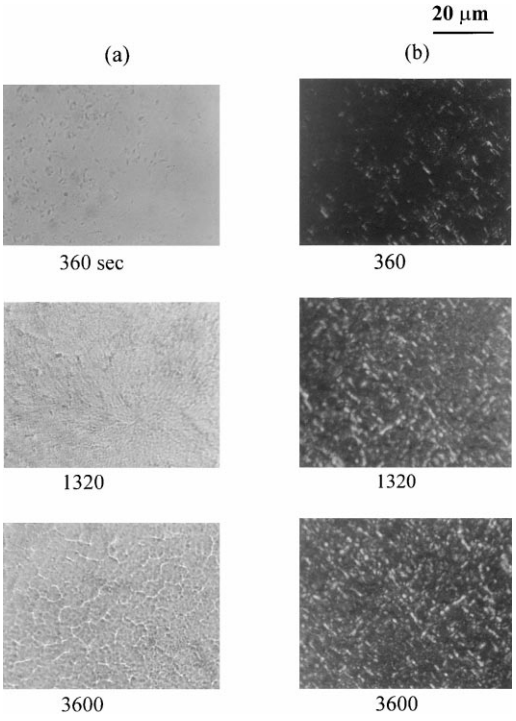

Fig. 6. Spatio-temporal growth of interconnected phase-separated domains during a *T* quench from a single-phase (128°C) to a two-phase temperature of 100°C below T_m; (a) unpolarized and (b) polarized conditions.

of thermally induced phase separation above the LCST as well as VIPS. The emergence of phase separation following *T* jumps into the LCST has been examined by means of optical microscopy by rapidly transferring the 50/50 sPP/EPDM blend from a single-phase temperature of 128°C to a two-phase region (i.e. 175°C). As shown in Fig. 5, multiple tiny interconnected structures develop spontaneously and coarsen with elapsed time. A similar study was conducted by transferring the 50/50 blend from a single-phase (128°C) to a two-phase temperature of 100°C below the T_m as well as the UCST coexistence temperature. Fig. 6 exhibits the temporal emergence of phase separated domains under (a) parallel and (b) crossed polarizers. Tiny structures develop which are seemingly birefringent under crossed polarizers (Fig. 6b). It appears that the liquid–liquid phase separation may be competed by the crystallization of sPP in the blends. One drawback in dealing with the sPP crystallization is that the crystalline morphology of sPP does not develop into a well-defined spherulitic structure, and therefore is not well resolved under the microscopic investigation. To avoid the implication of crystallization on liquid–liquid phase separation, we shall first focus on the dynamics of phase separation within the LCST.

In order to mimic the dynamics of phase separation, time-resolved light scattering experiments were undertaken at the same 50/50 composition by undertaking several *T* jumps into the LCST immiscibility gap. Fig. 7 shows temporal evolution of scattering profiles following several *T* jumps from a single-phase temperature of 128°C into various temperatures of 145, 160 and 170°C within the LCST. A scattering maximum appears in all *T* jumps and shifts gradually to a lower scattering angle with elapsed time, suggestive of domain growth. There is no period that is identifiable with the early stage of spinodal decomposition (SD). It seems, although by no means a proof, that the phase separation process may be dominated by the intermediate to late stage of SD. The growth dynamics in the intermediate or late stages of SD may be best characterized in terms of a power law scheme [10]

$$q_m(t) \propto t^{-\alpha} \tag{1}$$

$$I_m(t) \propto t^{\beta} \tag{2}$$

where the scattering maximum is defined as, $q_m = (4\pi/\lambda)\sin(\theta_m/2)$ with λ and θ being the wavelength of

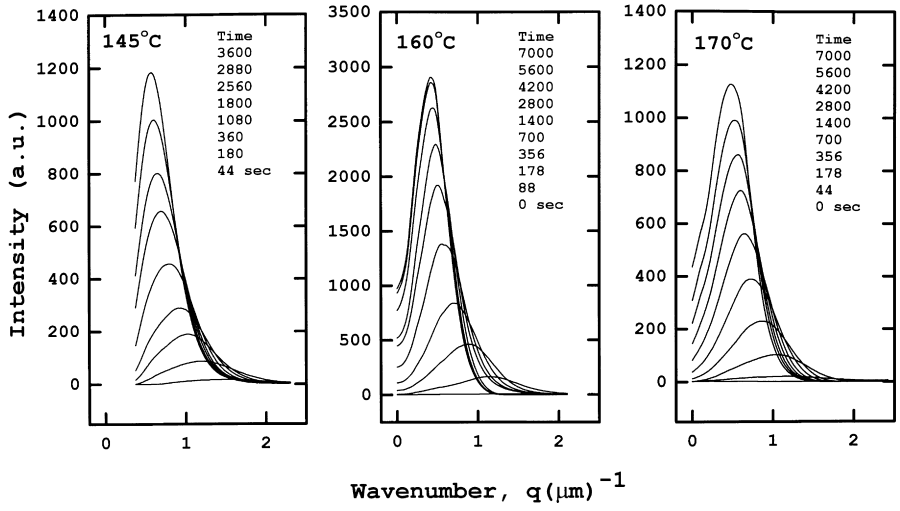

Fig. 7. Temporal evolution of scattering profiles following *T* jumps from a single phase (128°C) into various temperatures: 145, 160 and 170°C within the LCST.

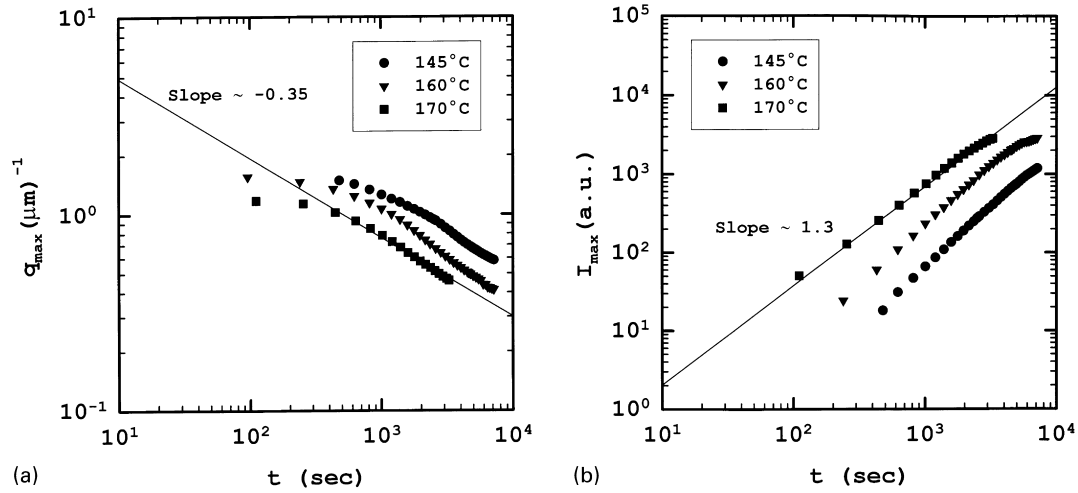

Fig. 8. Log–log plots of the 50/50 sPP/EPDM blends showing: (a) the scattering wavenumber maxima; and (b) the corresponding maximum intensity peak versus phase separation time.

light and the scattering angle measured in the medium, respectively. I_m is the corresponding scattering peak intensity.

Fig. 8a shows the log–log plot of scattering wavenumber versus phase separation time. The change of q_m is weak during the initial period, but it follows the power law growth with a slope of about $-1/3$ in the intermediate stage. In Fig. 8b, the corresponding plot of $I_m(t)$ versus t shows the power law growth with the slopes varying from 1.3 to 1.5. Judging from the relationship between the two exponents, i.e. $\beta > 3\alpha$ the phase demixing is dominated by the intermediate stage of SD.

A similar study has been extended to off-critical compositions such as the 70/30 and 30/70 sPP/EPDM blends, but the T jump was undertaken from 128 to 175°C only. One implication in the off-critical jumps is that nucleation and growth might occur especially in shallow quenches. The NG process generally proceeds through a heterogeneous nucleation process, therefore the distribution of droplets often leads to diffuse scattering without a clear maximum and hence the scattering results are difficult for quantification. If the T quench were sufficiently steep (for instant, the present case), SD would prevail over the NG, which in turn gives rise to a diffuse but definitive scattering halo in the scattering experiment. As shown in Fig. 9a, the temporal variation of q_m in the initial period is very small, but later it varies with a growth exponent ranging from -0.15 for the 30/70 blend to -0.3 for the 70/30 blend, which are smaller than those of the critical jumps. The reason for the observed smaller exponents in off-critical jumps is unclear at present, but this behavior has some resemblance to that of the VIPS to be discussed in a latter section. The corresponding I_m vs. t plot shows a slope of approximately 1.0 for the 30/70 blend and 1.5 for the 70/30 blend (Fig. 9b). Again the relationship

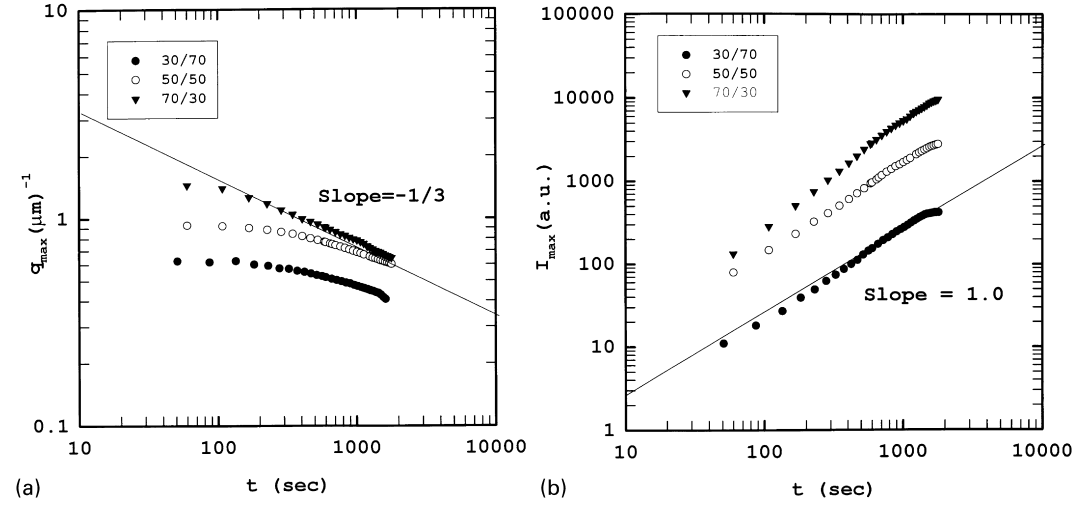

Fig. 9. Log–log plots of the 30/70 and 70/30 sPP/EPDM blends showing: (a) scattering wavenumber versus phase separation time; and (b) scattered intensity maximum versus phase separation time.

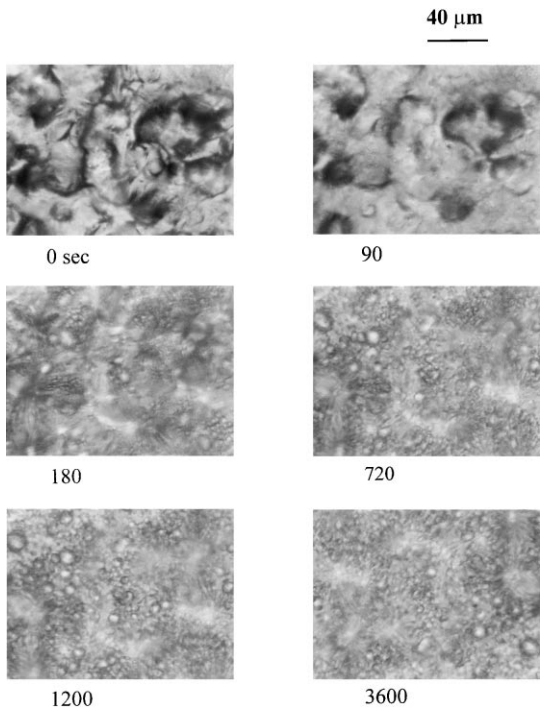

Fig. 10. Optical micrographs showing the temporal evolution of morphology of the 50/50 sPP/EPDM blends during vulcanization with the phenolic resin at 140°C.

$\beta > 3\alpha$ holds, which in turn implies the intermediate stage of SD. A similar growth behavior has been observed for the off-critical iPP/EPDM blends [14]. The observed growth behavior of liquid–liquid phase separation within the LCST of the sPP/EPDM blends is very similar to that of the conventional amorphous–amorphous mixtures. This finding is not surprising, in view of the fact that sPP/EPDM blends in the vicinity of the LCST are practically in the melt. Nevertheless, the present time-resolved light scattering study positively confirms the existence of the LCST reported earlier [8].

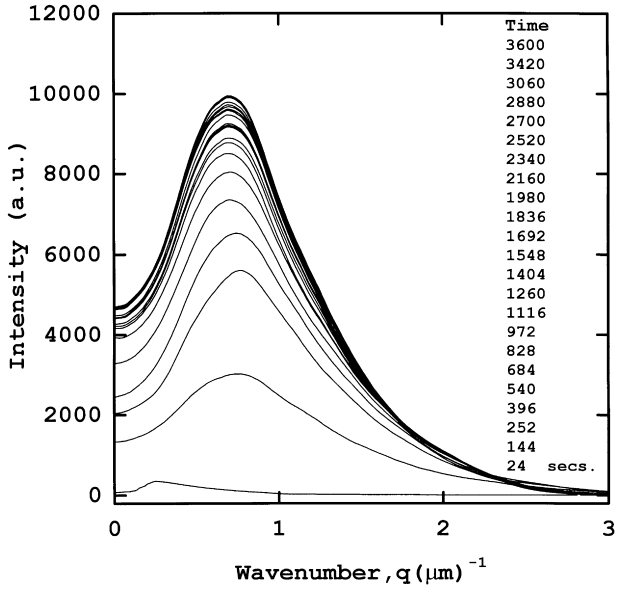

Fig. 11. Temporal evolution of the scattering curves of the 50/50 sPP/EPDM blends during vulcanization with the phenolic resin at 140°C.

3.3. Vulcanization induced phase separation

It has been a general practice to cross-link the blends of PP and EPDM by reacting the unsaturated bonds of the ENB with a phenolic resin [1–6]. It is of interest to investigate how the morphology of the PP/EPDM blend is influenced by the cross-linking reaction. The cure reaction (often called vulcanization) has been undertaken on various blends of sPP/EPDM using the phenolic resin. Fig. 10 depicts the changing morphology of the 50/50 sPP/EPDM blends during curing with the phenolic resin at 140°C. The sPP crystals begin to melt in 90 s and the crystal melting is seemingly completed around 180 s. Concurrently, the development of the phase-separated domains can be discerned in the background. With elapsed time, more droplets form in between the existing ones and become more populated (see the picture at 720 s). With continued reaction, these droplets seem fixed (see the picture at 3600 s) suggestive of the chemical cross-linking.

As it is not trivial to quantify the growth kinetics from the optical micrographs alone, time-resolved light scattering was undertaken during VIPS. Fig. 11 shows the temporal evolution of the scattering curves of the 50/50 sPP/EPDM blends using the phenolic resin during isothermal curing at 140°C. The initial sPP crystals melt and get homogenized with EPDM as this vulcanization temperature corresponds to the single-phase temperature of the sPP/EPDM. After a certain induction period (i.e. 144 s), a scattering peak first appears around a q of 0.8 μm and gradually shifts very slightly to a smaller wavenumber. A similar experiment was undertaken at various temperatures (130, 133, 148 and 155°C, all in a single-phase region). It may be postulated that the VIPS at low reaction temperatures such as 130 and 133°C may be driven by the upward shift of the UCST due to the proximity of the reaction temperature and the UCST coexistence curve. On the same token, the VIPS at high reaction temperatures such as 148 and 155°C may be driven predominantly by the downward shift of the LCST during cross-linking. At the intermediate reaction temperature of 140°C, phase separation seems to be affected by both the upward shift of UCST and the downward shift of LCST.

As shown in Figs. 12a and b, the change of q_m versus reaction time is very small relative to the thermal quench at the critical composition. At low reaction temperatures, the vulcanization rate is small, so the structural growth due to the thermal relaxation could dominate; thus one can discern the domain size to increase. When vulcanization commences at a later time, the domains can no longer grow because of the cross-linking reaction. The structural growth

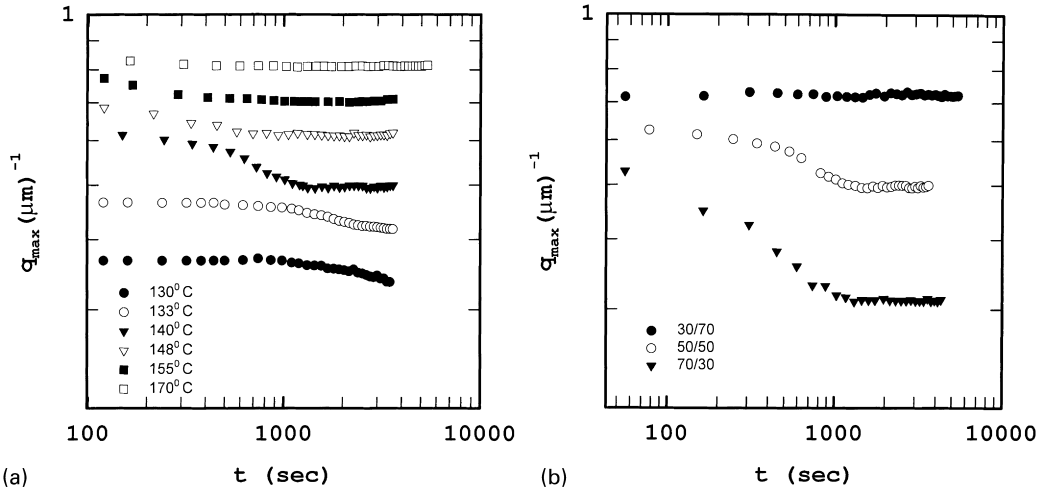

Fig. 12. Change of scattering wavenumber maxima versus reaction time: (a) at various vulcanization temperatures for the curing of the 50/50 sPP/EPDM; and (b) at various compositions using the phenolic resin as a curing agent.

becomes less distinct at high vulcanization temperatures due to the domination of the curing reaction, thereby chemically fixing the size of the domains. One notable observation is that the curing at elevated temperatures gives a smaller domain size. This trend is true even when vulcanization was carried out in the two-phase region at 170°C (i.e. above the LCST), suggesting the prevalence of the reaction kinetics.

One possible explanation for the observed small scaling exponent is that in VIPS the inter-domain distances get smaller as newer domains are formed between the existing ones so that the q_m increases with time [15,16]. Another important feature of VIPS is that the difference between the coexistence point and the reaction temperature becomes larger due to the progressive shift of the UCST to a higher temperature (or the LCST to a lower temperature) by virtue of increasing molecular weight. The VIPS tends to afford smaller domain sizes because of the notion that the larger the supercooling the smaller the domain size. Moreover, the increase in molecular weight will increase viscosity and hence slower diffusion; therefore the domain growth will slow down. On the other hand, the structural growth due to the coalescence driven by thermal relaxation will drive the q_m to decrease in time. These two opposing mechanisms would naturally cancel out each other or give a smaller growth exponent, which is exactly what has been observed in the present VIPS case. At longer times, the growth is inhibited by the cross-linking reaction, thereby arresting all structural growth due to the restricted mobility of the network chains.

It should be pointed out that a more drastic behavior has been first observed in the blends of carboxyl terminated butadiene acrylonitrile/diglycidyl ether bisphenol A epoxy/methylene dianiline experimentally. The instability of the reacting system was driven by the increase in molecular weight of the epoxy that drives the UCST to a higher temperature. When the UCST surpasses the reaction temperature, it does so at an off-critical composition, thereby passing through the metastable region to the unstable region [15]. Phase separation occurs through the nucleation and growth in the metastable, then crossing over to the unstable region where SD is dominant. This process was termed nucleation initiated spinodal decomposition (NISD) [15] so that it can be distinguished from the conventional SD. Another interesting feature of NISD is that the progressive increase of supercooling i.e. the temperature difference between the reaction temperature and the shifting UCST driven by the increase in molecular weight tends to make the domain size smaller. Note that the larger the supercooling, the smaller the average length scale.

In the present case of VIPS, NISD makes the length scale to be smaller while the thermally driven phase separation in approaching the equilibrium favors the domain growth. Depending on the relative rates of chemical reaction and phase growth, the final morphology may be determined. The observed trend of small growth exponents in the present system implies that the dynamics of phase separation and kinetics of chemical reaction may be comparable, in particular at higher reaction temperatures. When a three-dimensional network forms due to progressive vulcanization, the network structure is fixed permanently and no growth can be anticipated.

4. Conclusions

We have established the phase diagram of sPP/EPDM blends. In the order of descending temperature, the phase diagram reveals thermally reversible LCST followed by a single-phase region. At a lower temperature, the melting point depression of sPP occurs in the blends. With continued cooling a UCST is present in the sPP/EPDM blends which is intersected by the crystallization curve, showing the coexistence of crystal solid–liquid region. Of particular

interest is that the sPP/EPDM blends exhibit an LCST-type coexistence curve about 25–35°C above the T_m of sPP. The dynamics of liquid–liquid phase separation following T jumps into the LCST immiscibility gap reveals typical growth behavior with the exponents of approximately 1/3. The growth exponents in the VIPS turned out to be smaller than that of the thermal jump case. This observed small growth exponent may be attributed to the competition between the reduction of length scale driven by the reaction kinetics and the domain coarsening due to coalescence driven by thermal relaxation. One important observation within the temperature range investigated is that the higher the reaction temperature the smaller the domain size.

References

[1] Coran AY. In: Bhowmick AK, Stevens HL, editors. Handbook of elastomers: new developments and technology, New York: Marcel Dekker, 1988.
[2] Coran AY, Patel R. Rubber Chem Technol 1980;53:141.
[3] Coran AY, Patel R. Rubber Chem Technol 1980;53:781.
[4] Coran AY, Patel R. Rubber Chem Technol 1981;54:892.
[5] Coran AY, Patel R. Rubber Chem Technol 1983;56:210.
[6] Goettler LA, Richwine JR, Wille FJ. Rubber Chem Technol 1982;55:1558.
[7] Hashimoto T, Inaba N, Sato K, Suzuki S. Macromolecules 1986;19:1690.
[8] Chen CY, Yunus MZ, Chiu H-W, Kyu T. Polymer 1997;38:4433.
[9] Inoue T. Prog Polym Sci 1995;20:119.
[10] Gunton J, San Miguel M, Sahni PS. In: Domb C, Lebowitz JL, editors. Phase transitions and critical phenomena, 8. 1983. p. 269 chap 3.
[11] Saldanha JM, Kyu T. J Polym Sci Polym Lett Ed 1988;26:33.
[12] Wunderlich B. Macromolecular physics: crystal melting, 3. New York: Academic Press, 1980.
[13] Ramanujam A. MS thesis. University of Akron, Akron, Ohio 1998.
[14] Chen CY. MS thesis. University of Akron, Akron, Ohio 1993.
[15] Kyu T, Lee JH. Phys Rev Lett 1996;76:3746.
[16] Yamanaka K, Takagi Y, Inoue T. Polymer 1989;30:1989.